Fluid Dynamics and Co-located Conferences
June 24-27, 2013, San Diego, CA
21st AIAA Computational Fluid Dynamics Conference

A hybrid adjoint approach applied to turbulent flow simulations

Thomas W. R. Taylor*, Francisco Palacios†,
Karthik Duraisamy‡, and Juan J. Alonso§
Department of Aeronautics & Astronautics
Stanford University, Stanford, CA, 94305, U.S.A.

Adjoint-based techniques can provide the sensitivity of an objective function to any number of parameters of a simulation inexpensively at roughly the cost of a single additional flow calculation. This information can be used to perform sensitivity analyses, aerodynamic shape optimization, and to estimate the error in the objective function due to numerical discretization. Existing approaches to derive the numerically discretized adjoint equations involve the so-called discrete and continuous methods, which differ in the order at which discretization and linearization steps are performed. The effect of these contrasting approaches is that they have both strengths and weaknesses over each other in the form of complexity of the formulation and computational expense of the solution. In this paper, we further develop the hybrid approach of Taylor et al. (2012) that combines elements of the continuous and discrete methods with the intention of capturing both their advantages: reducing the time spent on mathematical derivation of the continuous adjoint equations, lowering the computational requirements of the discrete adjoint equations, and generally improving the quality of the adjoint solution. The specific approach investigated in this paper treats the flow conservation equations in a continuous manner and the turbulence transport equations discretely. The framework is designed such that additional transport equations for any turbulence model can be seamlessly included in a discrete fashion for coupling with the mean flow equations. The methodology is demonstrated in an optimization problem of lift-constrained drag minimization of an airfoil in transonic turbulent flow.

Nomenclature

Abbreviations

AD	= Automatic/Algorithmic Differentiation
ADOL-C	= Automatic Differentiation by Overloading in C++
AGARD	= Advisory Group for Aerospace Research and Development
CPU	= Central Processing Unit
CFD	= Computational Fluid Dynamics
PDE	= Partial Differential Equation
RAE	= Royal Aeronautical Establishment (U.K.)
RANS	= Reynolds-Averaged Navier-Stokes
SA	= Spalart-Allmaras turbulence model
SU^2	= Stanford University Unstructured code

Subscript and Superscript Definition

$()_{i,j,k,l}$	= Spatial components, 1 to 3. Repeated index implies summation
$()_{p,q,r}$	= Cell identifiers

*Ph.D. Candidate, AIAA Member
†Engineering Research Associate, AIAA Senior Member
‡Consulting Assistant Professor, AIAA Member
§Associate Professor, AIAA Associate Fellow

$()_C$ = Variable treated in continuous manner
$()_D$ = Variable treated in discrete manner
$()_H$ = Variable treated in hybrid manner
$()_L$ = Term from mean flow
$()_S$ = Value on wall boundary
$()_T$ = Term from turbulence model
$()_{\mu_T}$ = Term from eddy viscosity equation
$()_\rho$ = Variable related to density
$()_{\rho E}$ = Variable related to energy
$()_{\rho u_i}$ = Variable related to ith component of momentum
$()_\Gamma$ = Value/operator on boundary
$()_{\Gamma_\infty}$ = Value on far field boundary
$()_\Omega$ = Value/operator in domain

Variable Definition

c = Speed of sound
c_{b1} = Spalart-Allmaras model constant
c_{b2} = Spalart-Allmaras model constant
c_{w1} = Spalart-Allmaras model constant
d = Distance from nearest wall
f = Function for eddy viscosity
f_{v1} = Spalart-Allmaras model term
f_{v2} = Spalart-Allmaras model term
f_w = Spalart-Allmaras model term
g = Spalart-Allmaras model term
j_Γ = Integrand of surface integral in objective function
j_Ω = Integrand of domain integral in objective function
n = Number of incoming characteristics
$\hat{n}$ = Normal vector
p = Static pressure
r = Spalart-Allmaras model term
t = Time coordinate
u = Flow velocity
x = Spatial coordinates
C = Constant in exponential combustion source term
C_p = Specific heat capacity under constant pressure
E = Internal energy
F = Convective flux
F^{v1} = First viscous flux term
F^{v2} = Second viscous flux term
G = Adjoint flux term
H = Stagnation enthalpy
L = Primal problem linear operator
L^* = Adjoint problem linear operator
M = Mach number
N = Total number of cells/number of cells on coarse grid
Pr = Laminar Prandtl number
Pr_T = Turbulent Prandtl number
R = Gas constant
S = Wall boundary
$\hat{S}$ = Spalart-Allmaras model term
T = Static temperature
T^{cv} = Spalart-Allmaras turbulence model flux term
T^s = Spalart-Allmaras turbulence model source term
U = Vector of conservative flow variables

W = Characteristics
$(W)_+$ = Incoming characteristics
W_∞ = Characteristics at the far field
$\mathcal{A}_i,\ \mathcal{B}_i,\ \mathcal{C}_i$ = Substitutions used to simplify mathematical working
$\mathcal{G}$ = Governing equations
$\mathcal{J}$ = Objective function
$\mathcal{L}$ = Lagrangian
$\mathcal{N}$ = Analytical governing equations
$\mathcal{R}$ = Numerical residual
$\mathcal{R}^*$ = Numerical residual in a boundary cell minus the flux across the boundary
$\mathcal{R}^{(*)}$ = General symbol for $\mathcal{R}$ (internally) or $\mathcal{R}^*$ (on boundary)
α = General parameter under which perturbation is considered
β = Switching variable in hybrid objective function
γ = Ratio of specific heats
κ = Spalart-Allmaras model constant
μ = Laminar viscosity
μ_1 = First constant in Sutherland's law
μ_2 = Second constant in Sutherland's law
μ_T = Turbulent viscosity
μ^{v1} = First viscosity combination
μ^{v2} = Second viscosity combination
ν = Kinematic viscosity
$\hat{\nu}$ = Spalart-Allmaras turbulence model variable
ρ = Density
σ = Spalart-Allmaras model constant
τ = Stress tensor
ϕ = Continuous adjoint variable
φ = Hybrid adjoint variable
χ = Spalart-Allmaras model term
ψ = Discrete adjoint variable
ω = Vorticity
Γ = Flow domain boundary
Γ_p = Cell domain boundary
Γ_∞ = Far field boundary
Λ = Combustion progress variable
Ω = Flow domain
Ω_p = Cell domain

Mathematical Notation

$\emptyset$ = Empty set
$\{\}$ = Set of
$()'$ = Perturbed value
$\widehat{()}$ = Numerical flux
$()^T$ = Transpose
$\delta()$ = Dirac delta function
δ_{ij} = Kronecker delta function
$\mathcal{H}()$ = Heaviside function
$\delta()$ = Continuous perturbation
$\Delta()$ = Discrete perturbation
$\{\delta, \Delta\}()$ = Hybrid perturbation
$\partial_i()$ = Gradient in x_i direction, i.e., $\frac{\partial()}{\partial x_i}$
$\frac{\partial()}{\partial()}$ = Analytical Jacobian
$\frac{\mathfrak{D}()}{\mathfrak{D}()}$ = Numerical Jacobian

ϵ_{ijk} = Levi-Civita tensor

I. Introduction

Since being first introduced to aerodynamic applications by Jameson[1] in the late 1980s, adapting ideas from more general work by Lions[2] on optimal control of systems governed by partial differential equations (PDEs), the adjoint method has been used in a wide variety of areas. These include shape optimization of wing geometries,[3–6] sensitivity analysis[7,8] , uncertainty quantification[9–12] and goal-oriented numerical error estimation and mesh adaptation.[13–18]

Traditionally there are two different approaches to formulating the numerical system of adjoint equations: the discrete method, which derives the adjoint equations from the discretized residual equations used to numerically solve for the flow, and the continuous method, which starts from the continuous form of the governing equations, and only discretizes the problem when finally solving the continuous adjoint equations. Figure 1 illustrates the difference between these two approaches.

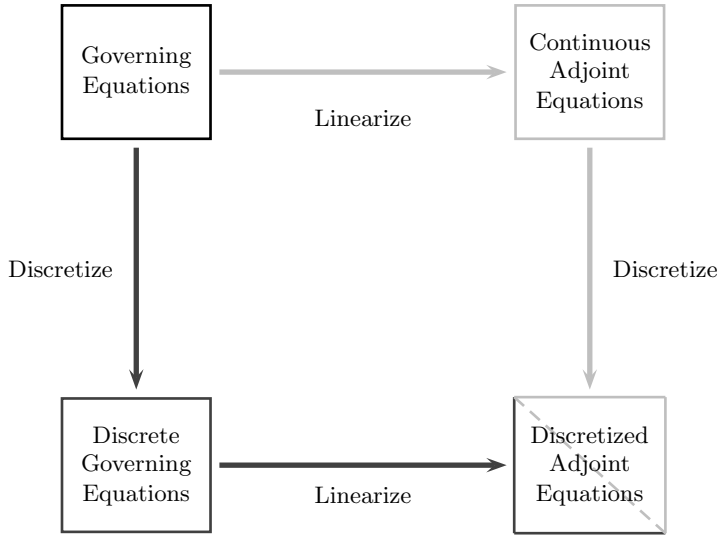

Figure 1. General scheme for discrete and continuous adjoints

Both these techniques are found to have relative advantages and disadvantages over each other. In theory, a discrete method can handle PDEs of arbitrary complexity without significant mathematical development and can treat arbitrary functionals. However, this method requires the evaluation of discrete Jacobians, which we denote as $\frac{\mathfrak{D}()}{\mathfrak{D}()}$ to distinguish from their continuous alternatives $\frac{\partial()}{\partial()}$, and there are two main ways to do this. The first is to analytically derive these terms from the discretized forms of the flow residuals and then develop code based on this, and the second is to use algorithmic Automatic Differentiation (AD), either via source code transformation[19] or operator overloading.[20] The former, analytical, approach requires significant development, more than that generally required in the continuous method,[21] while the latter can be computationally expensive.

In comparison, the continuous adjoint method requires significant theoretical development but is better connected to the underlying physics and can be solved in a method independent of the flow solution scheme. However, it is more limited in the types of functionals and governing equations that can be treated, and the gradient calculated will differ more substantially from the discrete gradient (which can be accurately computed by the discrete adjoint method), though, as the mesh is refined, both gradients should converge.

Taylor et al.[22] considered using a third, hybrid approach, that combines elements of both the discrete and continuous methods, deriving the adjoint equation from a mixture of the discretized residual equations and the continuous governing equations.[22] This general hybrid approach is illustrated in Figure 2.

In this paper we build on that previous work, which used quasi-one-dimensional flow with a combustion

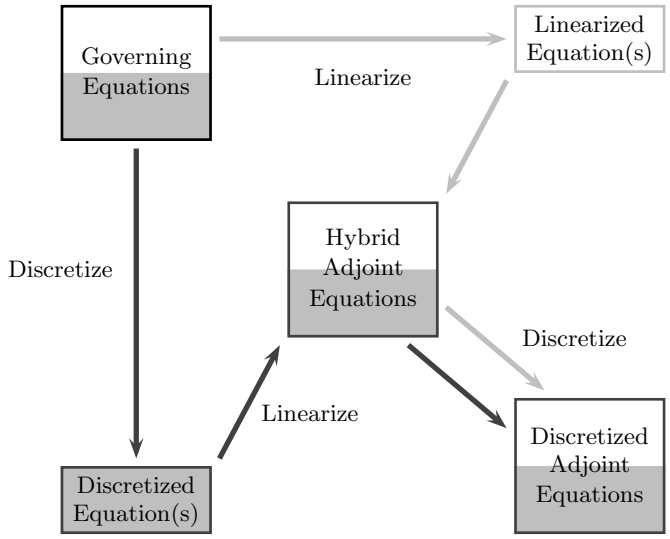

Figure 2. General scheme for a continuous–discrete adjoint hybrid

model as a test case, and extend the theory to handle two- and three-dimensional turbulent flows. To demonstrate one of the key advantages of this new approach we develop a hybrid method in which the continuous part, the mean flow, is model-independent. This means that the turbulence model can be switched without incurring additional development cost, noting that the intention is always to handle the discrete parts using AD. Also, it allows this model to be applied in situations where the turbulence model may be difficult or impossible to handle via the continuous adjoint approach.

To investigate the properties of the hybrid adjoint, application is extended to a case of an airfoil in transonic turbulent flow.[23,24]

Table 1 shows the relative advantages and disadvantages of the three different adjoint methods. Where an approach has been given a + sign this indicates it has favorable characteristics in this respect, and a − sign indicates undesirable characteristics. A ± sign indicates that the approach has been seen to fall somewhere in the middle and a question mark shows that further investigation is required.

	Discrete	Continuous	Hybrid
Ease of development[21,22,25–27]	+	−	±
Compatibility of numerical gradients:			
- with the discretized PDE[9,21,26–28]	+	−	−
- with the continuous PDE[26,29]	−	+	+
Surface formulation for gradients[28,30]	−	+	+
Ability to handle:			
- arbitrary functionals[22,27]	+	−	±
- non-differentiability[22,26,27,31]	+	−	+
Computational cost[13,21,26,27]	−	+	±
Flexibility in solution[21,22,26,29,32]	−	+	±

Table 1. Simple comparison between the discrete, continuous and hybrid adjoint approaches

Section II provides a general introduction to the adjoint method, including the discrete, continuous and hybrid approaches. Section III then introduces the Favre-Averaged Navier-Stokes equations, which are then used to develop the general turbulent hybrid adjoint in section IV. Results and discussion of the application of the hybrid adjoint method to the optimization of transonic turbulent flow over airfoils is presented in the

final section.

II. Introduction to adjoint methods

Adjoint equations can be conveniently formulated in a framework to calculate the sensitivity of a given objective function, $\mathcal{J}$, to parameters, α, in a problem governed by the set of equations which can be represented by $\mathcal{G}(U,\alpha)=0$, where U is the primal solution.

The adjoint variables can be used purely as a mathematical tool to find the required sensitivities, but, as discussed by Giles and Pierce[26] and Belegundu and Arora,[33] they can also be interpreted as representing the sensitivity of the objective function to perturbations in the governing equations, or the influence on the objective function of an arbitrary source function.

The additional computational cost of solving the adjoint problem is typically of the order of one additional flow solution,[34] and the adjoint variables represent the sensitivities of $\mathcal{J}$ to changes in all of the parameters that define the problem at every point in the domain. In contrast, though finite difference methods can also be used to find these sensitivities, they are in general significantly more expensive, requiring at least one additional flow solution to find the gradient of the objective function to any parameter in the domain. There are two main approaches used to derive the adjoint equations: the Primal-Dual Equivalence Theorem and an optimization framework using Lagrange multipliers.[26,33] In this paper, we consider the latter method, and, using this, handle the discrete and continuous parts of the hybrid adjoint derivation in an identical context. The following sections summarize the three different methods via this approach, but for a more complete discussion see Taylor.[22,35,36]

A. Discrete adjoint approach

In the discrete adjoint approach, the governing equations that we wish to enforce are the residuals, at every point in the domain, from the flow solution, $\mathcal{R}_p$, i.e., $\mathcal{G}=\{\mathcal{R}_p\}=0$. This gives the Lagrangian

$$\mathcal{L}=\mathcal{J}_D+\sum_{p=1}^{N}\psi_p^T\mathcal{R}_p, \tag{1}$$

where ψ are the Lagrange multipliers, or discrete adjoint variables, and the discrete perturbation to $\mathcal{L}$ is

$$\Delta\mathcal{L}=\Delta\mathcal{J}_D+\sum_{p=1}^{N}\psi_p^T\Delta\mathcal{R}_p. \tag{2}$$

After expanding and manipulating terms we define the adjoint equation, so as to remove the dependence on the flow perturbation, as

$$\sum_{q=1}^{N}\left(\frac{\mathfrak{D}\mathcal{R}_q}{\mathfrak{D}U_p}\right)^T\psi_q=-\left(\frac{\mathfrak{D}\mathcal{J}_D}{\mathfrak{D}U_p}\right)^T, \tag{3}$$

where we define the discrete Jacobian to be $\frac{\mathfrak{D}()}{\mathfrak{D}()}$, and the perturbation to the objective function is now

$$\Delta\mathcal{J}_D=\sum_{p=1}^{N}\psi_p^T\frac{\mathfrak{D}\mathcal{R}_p}{\mathfrak{D}\alpha}\Delta\alpha+\frac{\mathfrak{D}\mathcal{J}_D}{\mathfrak{D}\alpha}\Delta\alpha, \tag{4}$$

where it is seen that once the discrete adjoint equations (3) are solved, we can determine sensitivities of the objective function to any α relatively cheaply, needing only to consider the explicit dependence of $\mathcal{J}$ and $\mathcal{R}$ on α.

B. Continuous adjoint approach

In the continuous adjoint approach, we enforce the analytical form of the flow equations, $\mathcal{N}$, i.e., $\mathcal{G}=\{\mathcal{N}\}=0$. The Lagrangian is thus

$$\mathcal{L}=\mathcal{J}_C-\int_\Omega\phi^T\mathcal{N}d\Omega, \tag{5}$$

where ϕ are the Lagrange multipliers, or continuous adjoint variables, and the continuous perturbation to this now becomes

$$\delta\mathcal{L} = (\mathcal{J}'_C - \mathcal{J}_C) - \left(\int_{\Omega'} \phi^T \mathcal{N}' d\Omega - \int_{\Omega} \phi^T \mathcal{N} d\Omega\right), \tag{6}$$

where we note that perturbations to the parameter α may cause perturbations to both the flow, U, and the domain, Ω, and its bounding surface, Γ.

The next step is again to manipulate and rearrange terms such that the direct dependence of this quantity on the flow perturbations, δU, is removed, whilst retaining those terms dependent on perturbations to α and/or the domain and boundary surface. As these remaining terms are either known or easily determinable, the perturbation to the objective function can then readily be found with respect to those perturbations. This process will lead to the continuous adjoint equation and its boundary conditions, but its derivation and final form are intimately connected to the form of the governing equations, the flow boundary conditions and the objective function, and cannot be shown generally as in the discrete case above.

C. Hybrid adjoint approach

The main motivation behind a hybrid adjoint is to combine the best qualities of the discrete and continuous approaches. The general goal is to aim for the convergence and robustness properties of the continuous method, with the flexibility to handle arbitrarily complex PDEs of the discrete adjoint, but additional qualities of each, such as the existence of a surface formulation for gradients in the continuous adjoint approach, are also desirable. While there have been approaches that attempt to combine the continuous and discrete methods taken before, such as Lozano and Ponsin's post-processing use of continuous adjoint variables in a discrete adjoint framework to calculate sensitivities[29] and the approach by Giles et al. where continuous-like boundary conditions are used to improve the quality of the discrete adjoint solution near walls with strong boundary conditions,[37] the method discussed in this paper attempts to build a more general, true hybrid.

In our approach, we split the governing equations into those that will be enforced continuously and those that will be enforced discretely, i.e., $\mathcal{G} = \{\{\mathcal{N}\}_C, \{\mathcal{R}_p\}_D\} = 0$.

The equations that will be treated continuously will be those that will not change when making minor adjustments to the flow equations, such as when changing the source terms, and that are easily differentiable (e.g., the Euler equations for a perfect gas), whilst the terms treated discretely will include those that are not easily differential, and those that we may wish to change and experiment with (e.g., chemical source terms and turbulence models). One of the main intentions is that once the derivation for the continuous part is performed, substantial changes do not need to be made in the future, thus significantly lowering the development cost for additional problems.

Additionally, we define the objective function as one of either the discrete or continuous objective functions. We combine these by writing as a sum,

$$\mathcal{J}_H = \beta\mathcal{J}_C + (1-\beta)\mathcal{J}_D, \tag{7}$$

where β can be set equal to 0 or 1 in order to recover either the discrete or continuous functionals, respectively. Writing it in this way is useful so that both types of objective functions can be carried through the derivations simultaneously. It should be noted that it is also possible to create a weighted sum of both functionals, but that this has not been considered here. The idea of choosing between the discrete or continuous functionals is meant to allow us to choose the most suitable objective function for a specific problem, avoiding the disadvantages of the other, and a blend of both would therefore be counterproductive. However, one option not considered in this paper would be to switch between the discrete and continuous functionals at different points within the domain.

The Lagrangian now becomes

$$\mathcal{L} = \beta\mathcal{J}_C + (1-\beta)\mathcal{J}_D - \int_{\Omega} \varphi_C^T \mathcal{N}_C d\Omega + \sum_{p=1}^{N} \varphi_{D,p}^T \mathcal{R}_{D,p}, \tag{8}$$

where φ_C and φ_D are the Lagrange multipliers, or hybrid adjoint variables, and the hybrid perturbation can

thus be written as

$$\begin{aligned}\{\delta,\Delta\}\mathcal{L} &= \beta\left(\mathcal{J}'_C-\mathcal{J}_C\right)+(1-\beta)\Delta\mathcal{J}_D \\ &\quad -\left(\int_{\Omega'}\varphi_C^T\mathcal{N}'_C d\Omega-\int_{\Omega}\varphi_C^T\mathcal{N}_C d\Omega\right)+\sum_{p=1}^{N}\varphi_{D,p}^T\Delta\mathcal{R}_{D,p}.\end{aligned} \tag{9}$$

The next steps in this derivation are similar to those introduced previously for the discrete and continuous parts, mathematically manipulating the equation so as to remove the explicit dependence of the perturbation on δU, and in so doing generating the adjoint equation and boundary conditions for φ_C and φ_D. Due to the dependence of this method on the actual analytical form of the continuous part, this cannot be shown generally.

However, we can make a general observation about the hybrid boundary conditions. When solving the discrete adjoint equations, no such conditions need to be explicitly enforced, because they are already enforced within the calculation of the flow residuals. However, this is not the case for the hybrid approach, which now requires hybrid conditions relating the continuous, φ_C, and discrete, φ_D, variables from the hybrid adjoint solution. This more closely mirrors the fully continuous than fully discrete approach.

When deriving and calculating the hybrid adjoint for a specific problem, two important choices will need to be made. The first deals with exactly which governing equations are treated discretely and continuously, and the second is to decide whether to use the discrete or continuous objective function.

An interesting feature to be noted is that the discrete and continuous approaches are, in fact, special cases of the more general hybrid approach. By setting $\beta = 0$ and defining $\{\mathcal{R}\}_D = \mathcal{R}$, and thus $\{\mathcal{N}\}_C = \emptyset$, we recover the pure discrete method, and by setting $\beta = 1$ and defining $\{\mathcal{N}\}_C = \{\mathcal{N}\}$, and thus $\{\mathcal{R}\}_D = \emptyset$, we get the pure continuous.

However, we are no longer limited to just those two options. It is possible to create a continuous adjoint that has a discrete functional, allowing non-differentiable cost functions to be considered in the continuous approach, or vice versa, and many other combinations in between.

III. Governing equations of the primal problem

A. Definition

The governing equations considered in this paper are the standard Reynolds-Averaged Navier-Stokes equations[38] for compressible flow along with a required turbulence model, and together these can be written

$$\mathcal{N}(U,\partial_j U,\alpha)=\begin{pmatrix}\mathcal{N}_L\\ \mathcal{N}_T\end{pmatrix}=0,\quad \text{in } \Omega, \tag{10}$$

where the variables, U, consist of mean flow variables, U_L, and turbulence variables, U_T,

$$U=\begin{pmatrix}U_L\\ U_T\end{pmatrix}, \tag{11}$$

and $\partial_j U$ are the gradients of the flow variables and α is an undefined parameter that we wish to find sensitivities relative to.

1. *Reynolds-Averaged Navier-Stokes equations*

The mean flow equations are

$$\mathcal{N}_L(U,\partial_j U,\alpha)=\partial_i\left(F_i-\mu^{v1}F_i^{v1}-\mu^{v2}F_i^{v2}\right)=0,\quad \text{in } \Omega, \tag{12}$$

subject to the boundary conditions

$$\begin{aligned}&u_i=0, && \text{on } S,\\ &\hat{n}_i\partial_i T=0, && \text{on } S,\\ &(W)_+=W_\infty, && \text{on } \Gamma_\infty,\end{aligned} \tag{13}$$

where the mean flow variables are

$$U_L = \begin{pmatrix} \rho \\ \rho u_i \\ \rho E \end{pmatrix}, \tag{14}$$

and the convective and viscous flux vectors are given by

$$F_i = \begin{pmatrix} \rho u_i \\ \rho u_i u_j + p\delta_{ij} \\ \rho u_i H \end{pmatrix}, \quad F_i^{v1} = \begin{pmatrix} 0 \\ \tau_{ij} \\ u_k \tau_{ik} \end{pmatrix}, \quad F_i^{v2} = \begin{pmatrix} 0 \\ 0 \\ C_p \partial_i T \end{pmatrix}, \tag{15}$$

where the temperature and stress are

$$T = \frac{p}{R\rho}, \quad \tau_{ij} = (\partial_j u_i + \partial_i u_j) - \frac{2}{3}\delta_{ij}\partial_k u_k. \tag{16}$$

We also define the viscosity terms in eqn. (12) as

$$\mu^{v1} = \mu + \mu_T, \quad \mu^{v2} = \frac{\mu}{Pr} + \frac{\mu_T}{Pr_T}, \tag{17}$$

where Pr and Pr_T are the laminar and turbulent Prandtl numbers, respectively, and the laminar viscosity, μ, is given by Sutherland's law,

$$\mu = \frac{\mu_1 T^{\frac{3}{2}}}{T + \mu_2}. \tag{18}$$

Finally, the eddy viscosity, μ_T, is assumed to be the sole coupling term between the turbulence model and the mean flow equations, and the specific form of μ_T depends on the exact turbulence model being used.

2. *General turbulence model*

A set of governing equations for a general turbulence model can be written

$$\mathcal{N}_T(U, \partial_j U, \alpha) = \partial_i F_{T_i} - S_T = 0, \quad \text{in } \Omega, \tag{19}$$

where the flux, F_{T_i}, and source, S_T, may be functions of U, $\partial_j U$ and α.

The solution of this turbulence model will allow us to calculate the eddy viscosity, μ_T, which will then couple into the RANS governing equations (12) through the viscosity terms μ^{v1} and μ^{v2}. It is important to note that the form of μ_T will depend on the model being considered, but that it could generally be a function of U, $\partial_j U$ and α. However, one important boundary condition that applies to a general turbulence model is that on a viscous wall, $\mu_T = 0$.

3. *Spalart-Allmaras one-equation turbulence model*

The candidate turbulence model considered in this paper is the one-equation Spalart-Allmaras turbulence model,[39] which has the governing equation

$$\mathcal{N}_T(U, \partial_j U, \alpha) = \partial_i T_i^{cv} - T^s = 0, \quad \text{in } \Omega, \tag{20}$$

subject to the boundary conditions

$$\begin{aligned} \hat{\nu} &= 0, && \text{on } S, \\ \hat{\nu}_\infty &= \sigma_\infty \nu_\infty, && \text{on } \Gamma_\infty, \end{aligned} \tag{21}$$

where the convective flux is given by

$$T_i^{cv} = -\frac{\nu + \hat{\nu}}{\sigma}\partial_i \hat{\nu} + u_i \hat{\nu}, \tag{22}$$

and the source term is

$$T^s = c_{b1}\hat{S}\hat{\nu} - c_{w1} f_w \left(\frac{\hat{\nu}}{d_s}\right)^2 + \frac{c_{b2}}{\sigma}\left(\partial_i \hat{\nu}\right)\left(\partial_i \hat{\nu}\right). \tag{23}$$

We identify the turbulence flow variable for this model as

$$U_T = \hat{\nu}, \tag{24}$$

and note that the eddy viscosity is given by

$$\mu_T = \rho \hat{\nu} f_{v1}. \tag{25}$$

In the above formula we must define the following terms

$$\begin{aligned}
&f_{v1} = \frac{\chi^3}{\chi^3 + c_{v1}^3}, \quad \chi = \frac{\hat{\nu}}{\nu}, \quad \nu = \frac{\mu}{\rho}, \\
&\hat{S} = \sqrt{\omega_i \omega_i} + \frac{\hat{\nu}}{\kappa^2 d_s^2} f_{v2}, \quad \omega_k = \epsilon_{ijk} \partial_i u_j, \\
&f_{v2} = 1 - \frac{\chi}{1 + \chi f_{v1}}, \qquad f_w = g \left(\frac{1 + c_{w3}^6}{g^6 + c_{w3}^6} \right)^{\frac{1}{6}}, \\
&g = r + c_{w2}(r^6 - r), \qquad r = \frac{\hat{\nu}}{\hat{S} \kappa^2 d_s^2},
\end{aligned} \tag{26}$$

where the model constants are

$$\begin{aligned}
&\sigma = \frac{2}{3}, && c_{b1} = 0.1355, \\
&c_{b2} = 0.622, && \kappa = 0.41, \\
&c_{w1} = \frac{c_{b1}}{\kappa^2} + \frac{1 + c_{b2}}{\sigma}, && c_{w2} = 0.3, \\
&c_{w3} = 2, && c_{v1} = 7.1.
\end{aligned} \tag{27}$$

B. Solution strategy

The numerical solution method for the mean flow and turbulence equations was implemented in the open-source code SU^2.[40] For the mean flow, the convective terms were discretized using the Jameson-Schmidt-Turkel central-differencing scheme and the viscous terms were discretized by averaging the gradients and including a correction based on the directional derivative. For the selected turbulence model, the Spalart-Allmaras one-equation model, the convective terms were discretized using first order upwinding, the viscous terms were again handled by averaging the gradients and the source terms were treated in a piece-wise manner.

Within each major iteration of the flow solver, an implicit backward Euler scheme was used for the pseudo-time integration of the mean flow step and subsequently, the turbulence model step. It is to be noted that the coupling of the turbulence model into the mean flow is only through the eddy viscosity, while the turbulence model requires density, velocity and laminar viscosity information from the mean flow.

IV. Hybrid adjoint equations

A. Derivation

To derive a general set of hybrid adjoint equations for turbulent flow, we consider the hybrid objective function,

$$\mathcal{J}_H = \beta \left(\int_\Omega j_\Omega d\Omega + \int_\Gamma j_\Gamma d\Gamma \right) + (1 - \beta) \frac{\mathfrak{D} \mathcal{J}_D}{\mathfrak{D} \alpha} \Delta \alpha, \tag{28}$$

where by appropriate choice of β (0 or 1), we may select either a discrete or continuous objective function, and through definition of j_Ω, j_Γ and $\mathcal{J}_D$ the objective function may be defined in the domain, on the boundary, or both.

Also, one of the key goals of applying the hybrid adjoint approach to turbulent flow is that the mean flow equations can be handled continuously and turbulence models discretely. Using Automatic Differentiation to obtain the required terms in the discrete approach will then mean that the turbulence models can be treated as black boxes, and that the models can be switched in and out without the need to perform any additional analytical development. However, it can be seen in eqn. (17) that the viscosity terms in the mean

flow equations (eqn. 12) depend explicitly on the eddy viscosity, μ_T. Additionally, the form of μ_T depends on the exact turbulence model being used — e.g., the form for the Spalart-Allmaras one-equation turbulence model is given by eqn. (25) — and thus there is a model-dependence in the mean flow equations.

This model-dependence can, however, be removed by the introduction of a dummy governing equation for the eddy viscosity,

$$\mathcal{N}_{\mu_T}(U, \partial_j U, \alpha) = \mu_T - f = 0, \quad \text{in } \Omega, \tag{29}$$

where

$$f(U, \partial_j U, \alpha) = \mu_T. \tag{30}$$

Treating this dummy governing equation discretely will allow the explicit dependence on the form of the eddy viscosity to be moved from the continuous part of the hybrid adjoint equations to the discrete part.

We now enforce the mean flow governing equations, $\mathcal{N}_L$, and the eddy viscosity and turbulence model numerical residuals, $\mathcal{R}_{\mu_T}$ and $\mathcal{R}_T$, respectively, by introducing the modified Lagrangian

$$\begin{aligned} \mathcal{L} &= \beta \left(\int_\Omega j d\Omega + \int_\Gamma j_\Gamma d\Gamma \right) + (1-\beta) \frac{\mathfrak{D}\mathcal{J}_D}{\mathfrak{D}\alpha} \Delta\alpha \\ &\quad - \int_\Omega \varphi_C^T \mathcal{N}_L d\Omega - \sum_{p=1}^{N} \varphi_{\mu_{T_p}}^T \mathcal{N}_{\mu_{T_p}} \Delta\Omega_p + \sum_{p=1}^{N} \varphi_{D_p}^T \mathcal{R}_{T_p}, \end{aligned} \tag{31}$$

where $\varphi = \{\varphi_C, \varphi_{\mu_T}, \varphi_D\}$ are the Lagrange multipliers (or hybrid adjoint variables).

Taking the perturbation of the Lagrangian to a change in some parameter α we then get, after linearization and appropriate manipulation,

$$\begin{aligned} \{\delta, \Delta\}\mathcal{L} &= \int_\Omega \left(\beta \frac{\partial j}{\partial \alpha} \delta\alpha - \varphi_C^T \partial_i \left(\left(\frac{\partial F_i}{\partial \alpha} - \mathcal{A}_1 - \mathcal{A}_4 - \mathcal{B}_1 \right) \delta\alpha \right) \right) d\Omega \\ &\quad + \int_\Gamma \beta \frac{\partial j_\Gamma}{\partial \alpha} \delta\alpha d\Gamma + (1-\beta) \frac{\mathfrak{D}\mathcal{J}_D}{\mathfrak{D}\alpha} \Delta\alpha \\ &\quad + \sum_{p=1}^{N} \varphi_{\mu_{T_p}}^T \frac{\mathfrak{D} f_p}{\mathfrak{D}\alpha} \Delta\alpha \Delta\Omega_p + \sum_{p=1}^{N} \varphi_{D_p}^T \frac{\mathfrak{D}\mathcal{R}_{T_p}}{\mathfrak{D}\alpha} \Delta\alpha \\ &\quad - \int_\Omega \left(L_\Omega^*(\varphi_C) - \beta \left(\frac{\partial j_\Omega}{\partial U} \right)^T \right)^T \delta U d\Omega \\ &\quad - \int_\Gamma \left(\left(L_\Gamma^*(\varphi_C) - \beta \left(\frac{\partial j_\Gamma}{\partial U} \right)^T \right)^T \delta U - \varphi_C^T \left(\mathcal{A}_3 + \mathcal{B}_3 \right) \delta(\partial_j U) \hat{n}_i \right) d\Gamma \\ &\quad - \int_\Omega \left(\partial_i \varphi_C^T \right) \mathcal{C}_1 \delta\mu_T d\Omega + \int_\Gamma \varphi_C^T \mathcal{C}_1 \hat{n}_i \delta\mu_T d\Gamma \\ &\quad + (1-\beta) \sum_{p=1}^{N} \frac{\mathfrak{D}\mathcal{J}_D}{\mathfrak{D} U_p} \Delta U_p + \sum_{p=1}^{N} \sum_{q=1}^{N} \varphi_{D_q}^T \frac{\mathfrak{D}\mathcal{R}_{T_q}}{\mathfrak{D} U_p} \Delta U_p \\ &\quad + \sum_{p=1}^{N} \sum_{q=1}^{N} \varphi_{\mu_{T_q}}^T \frac{\mathfrak{D} f_q}{\mathfrak{D} U_p} \Delta U_p \Delta\Omega_q - \sum_{p=1}^{N} \varphi_{\mu_{T_p}}^T \Delta\mu_{T_p} \Delta\Omega_p, \end{aligned} \tag{32}$$

where the adjoint linear operators are

$$L_\Omega^*(\varphi_C) = -\left(\frac{\partial F_i}{\partial U} - \mathcal{A}_2 - \mathcal{A}_5 - \mathcal{B}_2 \right)^T \partial_i \varphi_C - \partial_j \left(\left(\mathcal{A}_3 + \mathcal{B}_3 \right)^T \partial_i \varphi_C \right), \tag{33}$$

and

$$L_\Gamma^*(\varphi_C) = \left(\left(\frac{\partial F_i}{\partial U} - \mathcal{A}_2 - \mathcal{A}_5 - \mathcal{B}_2 \right) \hat{n}_i \right)^T \varphi_C + \left(\left(\mathcal{A}_3 + \mathcal{B}_3 \right) \hat{n}_j \right)^T \partial_i \varphi_C, \tag{34}$$

and where we have introduced the substitutions,

$$\mathcal{A}_1 = \mu \left(\frac{\partial F_i^{v1}}{\partial \alpha} + \left(\frac{1}{Pr} \right) \frac{\partial F_i^{v2}}{\partial \alpha} \right), \tag{35}$$

$$\mathcal{A}_2 = \mu \left(\frac{\partial F_i^{v1}}{\partial U} + \left(\frac{1}{Pr} \right) \frac{\partial F_i^{v2}}{\partial U} \right), \tag{36}$$

$$\mathcal{A}_3 = \mu \left(\frac{\partial F_i^{v1}}{\partial (\partial_j U)} + \left(\frac{1}{Pr} \right) \frac{\partial F_i^{v2}}{\partial (\partial_j U)} \right), \tag{37}$$

$$\mathcal{A}_4 = \left(F_i^{v1} + \left(\frac{1}{Pr} \right) F_i^{v2} \right) \frac{\partial \mu}{\partial \alpha}, \tag{38}$$

$$\mathcal{A}_5 = \left(F_i^{v1} + \left(\frac{1}{Pr} \right) F_i^{v2} \right) \frac{\partial \mu}{\partial U}, \tag{39}$$

$$\mathcal{B}_1 = \mu_T \left(\frac{\partial F_i^{v1}}{\partial \alpha} + \left(\frac{1}{Pr_T} \right) \frac{\partial F_i^{v2}}{\partial \alpha} \right), \tag{40}$$

$$\mathcal{B}_2 = \mu_T \left(\frac{\partial F_i^{v1}}{\partial U} + \left(\frac{1}{Pr_T} \right) \frac{\partial F_i^{v2}}{\partial U} \right), \tag{41}$$

$$\mathcal{B}_3 = \mu_T \left(\frac{\partial F_i^{v1}}{\partial (\partial_j U)} + \left(\frac{1}{Pr_T} \right) \frac{\partial F_i^{v2}}{\partial (\partial_j U)} \right), \tag{42}$$

and

$$\mathcal{C}_1 = \left(F_i^{v1} + \left(\frac{1}{Pr_T} \right) F_i^{v2} \right). \tag{43}$$

The adjoint equations are then defined so as to remove the dependence of $\{\delta, \Delta\}\mathcal{L}$ on the flow and eddy viscosity perturbations. We can first remove the terms containing either $\delta\mu_T$ or $\Delta\mu_T$ from eqn. (32) by asserting that

$$\int_\Omega \left(\partial_i \varphi_C^T \right) \mathcal{C}_1 \delta\mu_T d\Omega + \sum_{p=1}^{N} \varphi_{\mu_{T_p}}^T \Delta\mu_{T_p} \Delta\Omega_p - \int_\Gamma \varphi_C^T \mathcal{C}_1 \hat{n}_i \delta\mu_T d\Gamma = 0. \tag{44}$$

Noting that at a true far field we can neglect the viscous flux contributions and that at a viscous wall the eddy viscosity is zero, and thus $\delta\mu_T = 0$, we can remove the boundary term from eqn. (44), giving,

$$\int_\Omega \left(\partial_i \varphi_C^T \right) \mathcal{C}_1 \delta\mu_T d\Omega + \sum_{p=1}^{N} \varphi_{\mu_{T_p}}^T \Delta\mu_{T_p} \Delta\Omega_p = 0. \tag{45}$$

Discretizing the domain integral into a sum of the integrals over each cell, and then making the assumption that this condition is not just true within the whole domain, but also within each cell, we obtain, for cell p,

$$\int_{\Omega_p} \left(\partial_i \varphi_C^T \right) \mathcal{C}_1 \delta\mu_T d\Omega + \varphi_{\mu_{T_p}}^T \Delta\mu_{T_p} \Delta\Omega_p = 0. \tag{46}$$

Now, under the assumption that $\delta\mu_T$ is step-wise constant within each cell, we may factor it out of the integral, and, if we also assume that $\delta\mu_{T_p} \approx \Delta\mu_{T_p}$, we may cancel out the dependence on the perturbation to the eddy viscosity, giving, after rearrangement,

$$\varphi_{\mu_{T_p}}^T \Delta\Omega_p = -\int_{\Omega_p} \left(\partial_i \varphi_C^T \right) \mathcal{C}_1 d\Omega. \tag{47}$$

Next, to remove the terms containing either δU or ΔU from eqn. (32) we write

$$\begin{aligned}
&\int_{\Omega} \left(L^*_{\Omega}(\varphi_C) - \beta \left(\frac{\partial j_{\Omega}}{\partial U} \right)^T \right)^T \delta U d\Omega \\
&+ \int_{\Gamma} \left(\left(L^*_{\Gamma}(\varphi_C) - \beta \left(\frac{\partial j_{\Gamma}}{\partial U} \right)^T \right)^T \delta U - \varphi_C^T \left(\mathcal{A}_3 + \mathcal{B}_3 \right) \delta(\partial_j U) \hat{n}_i \right) d\Gamma \\
&- (1-\beta) \sum_{p=1}^{N} \frac{\mathfrak{D} \mathcal{J}_D}{\mathfrak{D} U_p} \Delta U_p - \sum_{p=1}^{N} \sum_{q=1}^{N} \varphi_{D_q}^T \frac{\mathfrak{D} \mathcal{R}_{T_q}}{\mathfrak{D} U_p} \Delta U_p \\
&- \sum_{p=1}^{N} \sum_{q=1}^{N} \varphi_{\mu_{T_q}}^T \frac{\mathfrak{D} f_q}{\mathfrak{D} U_p} \Delta U_p \Delta \Omega_q \quad = \quad 0.
\end{aligned} \tag{48}$$

The boundary terms can be removed by requiring that

$$\begin{aligned}
&\int_{\Gamma} \left(\left(L^*_{\Gamma}(\varphi_C) - \beta \left(\frac{\partial j_{\Gamma}}{\partial U} \right)^T \right)^T \delta U - \varphi_C^T \left(\mathcal{A}_3 + \mathcal{B}_3 \right) \delta(\partial_j U) \hat{n}_i \right) d\Gamma \\
&- (1-\beta) \sum_{p=1}^{N_S} \sum_{q=1}^{N_S} \frac{\mathfrak{D} j_{\Gamma_q}}{\mathfrak{D} U_{T_p}} \Delta \Gamma_q \Delta U_{T_p} - \sum_{p=1}^{N_\Gamma} \sum_{q=1}^{N_\Gamma} \varphi_{D_q}^T \frac{\mathfrak{D} (\hat{F}_T)_{\Gamma_q}}{\mathfrak{D} U_p} \Delta U_p \quad = \quad 0,
\end{aligned} \tag{49}$$

where the boundary flux of the turbulence model has been separated out from the residual in order to create a fully hybrid boundary condition. This modification of the residual can be written as

$$\mathcal{R}_{T_p} = (\hat{F}_T)_{\Gamma_p} + \mathcal{R}^*_{T_p}. \tag{50}$$

We also note that the discrete objective function on the surface in eqn. (49) has been written as

$$\mathcal{J}_{D_\Gamma} = \sum_{q=1}^{N_S} j_{\Gamma_q} \Delta \Gamma_q. \tag{51}$$

At the far field, considering objective functions not defined along that boundary and neglecting flow gradients and viscosity contributions, eqn. (49) will reduce to the Euler far field boundary condition,

$$- \int_{\Gamma_\infty} \phi^T \frac{\partial F_i}{\partial U} \hat{n}_i \delta U d\Gamma = 0. \tag{52}$$

At the viscous wall, discretizing the surface integral in eqn. (49) into a sum of the integrals over the wall for each boundary cell, and then making the assumption that this condition is not just true over the whole surface, but also for each cell, we obtain, for cell p,

$$\begin{aligned}
&\int_{\Gamma_p} \left(\left(L^*_{\Gamma}(\varphi_C) - \beta \left(\frac{\partial j_{\Gamma}}{\partial U} \right)^T \right)^T \delta U - \varphi_C^T \left(\mathcal{A}_3 + \mathcal{B}_3 \right) \delta(\partial_j U) \hat{n}_i \right) d\Gamma \\
&- (1-\beta) \sum_{q=1}^{N_S} \frac{\mathfrak{D} j_{\Gamma_q}}{\mathfrak{D} U_{T_p}} \Delta \Gamma_q \Delta U_{T_p} - \sum_{q=1}^{N_\Gamma} \varphi_{D_q}^T \frac{\mathfrak{D} (\hat{F}_T)_{\Gamma_q}}{\mathfrak{D} U_p} \Delta U_p \quad = \quad 0,
\end{aligned} \tag{53}$$

After some manipulation, including the assumption that the perturbations in the flow quantities are

step-wise constant along the wall in each cell, this then becomes

$$\begin{aligned}
&\beta\left(\int_{S_p}\frac{\partial j_\Gamma}{\partial U}d\Gamma\right)\delta U_p+(1-\beta)\sum_{q=1}^{N_S}\frac{\mathfrak{D}j_{\Gamma_q}}{\mathfrak{D}U_p}\Delta\Gamma_q\Delta U_p\\
&-\left(\int_{S_p}\varphi^T_{C_{\rho u_j}}\hat{n}_i\right)\delta p_p+\sum_{q=1}^{N_S}\varphi^T_{D_q}\left(\frac{\rho_p}{p_p}\frac{\mathfrak{D}(\hat{F}_T)_{\Gamma_q}}{\mathfrak{D}\rho_p}+\frac{1}{\gamma-1}\frac{\mathfrak{D}(\hat{F}_T)_{\Gamma_q}}{\mathfrak{D}(\rho E)_p}\right)\Delta p_p\\
&+\left(\int_{S_p}\left(\varphi^T_{C_{\rho u_j}}\tau_{ij}\frac{\partial\mu}{\partial T}+\mu\left(\partial_i\varphi_{C_{\rho E}}\right)\frac{C_p}{Pr}\right)\hat{n}_i d\Gamma\right)\delta T_p-\sum_{q=1}^{N_S}\frac{\rho_p}{T_p}\varphi^T_{D_q}\frac{\mathfrak{D}(\hat{F}_T)_{\Gamma_q}}{\mathfrak{D}\rho_p}\Delta T_p\\
&+\left(\int_{S_p}\varphi^T_{C_{\rho u_j}}\mu\hat{n}_i d\Gamma\right)\delta\tau_{ij_p}\\
&+(1-\beta)\sum_{q=1}^{N_S}\frac{\mathfrak{D}j_{\Gamma_q}}{\mathfrak{D}U_{T_p}}\Delta\Gamma_q\Delta U_{T_p}+\sum_{q=1}^{N_S}\varphi^T_{D_q}\frac{\mathfrak{D}(\hat{F}_T)_{\Gamma_q}}{\mathfrak{D}U_{T_p}}\Delta U_{T_p} \quad = \quad 0,
\end{aligned}\tag{54}$$

which, given the additional assumption that the continuous perturbations are equal to the discrete ones, i.e., $\delta()_p \approx \Delta()_p$, implies that if the perturbation to the objective function can be written in the form

$$\frac{\partial j_\Gamma}{\partial U}\delta U=\frac{\partial j_\Gamma}{\partial p}\delta p+\frac{\partial j_\Gamma}{\partial \tau_{ij}}\delta\tau_{ij}+\frac{\partial j_\Gamma}{\partial T}\delta T+\frac{\partial j_\Gamma}{\partial U_T}\delta U_T,\tag{55}$$

the δp, $\delta\tau_{ij}$, δT and δU_T dependencies can be removed, producing adjoint boundary conditions on the wall.

With these boundary terms removed, and using eqn. (47) to remove the eddy viscosity adjoint variable, eqn. (48) becomes

$$\begin{aligned}
&\int_\Omega\left(L^*_\Omega(\varphi_C)-\beta\left(\frac{\partial j_\Omega}{\partial U}\right)^T\right)^T\delta U d\Omega\\
&-(1-\beta)\sum_{p=1}^{N}\frac{\mathfrak{D}\mathcal{J}_{D_\Omega}}{\mathfrak{D}U_p}\Delta U_p-\sum_{p=1}^{N}\sum_{q=1}^{N}\varphi^T_{D_q}\frac{\mathfrak{D}\mathcal{R}^{(*)}_{T_q}}{\mathfrak{D}U_p}\Delta U_p\\
&+\sum_{p=1}^{N}\sum_{q=1}^{N}\frac{\mathfrak{D}f_q}{\mathfrak{D}U_p}\Delta U_p\int_{\Omega_q}\left(\partial_i\varphi^T_C\right)\mathcal{C}_1 d\Omega \quad = \quad 0.
\end{aligned}\tag{56}$$

Discretizing the domain integral into a sum of the integrals over each cell, and then making the assumption that this condition is not just true within the whole domain, but also within each cell, we obtain, for cell p,

$$\begin{aligned}
&\int_{\Omega_p}\left(L^*_\Omega(\varphi_C)-\beta\left(\frac{\partial j_\Omega}{\partial U}\right)^T\right)^T\delta U d\Omega\\
&-(1-\beta)\frac{\mathfrak{D}\mathcal{J}_{D_\Omega}}{\mathfrak{D}U_p}\Delta U_p-\sum_{q=1}^{N}\varphi^T_{D_q}\frac{\mathfrak{D}\mathcal{R}^{(*)}_{T_q}}{\mathfrak{D}U_p}\Delta U_p\\
&+\sum_{q=1}^{N}\frac{\mathfrak{D}f_q}{\mathfrak{D}U_p}\Delta U_p\int_{\Omega_q}\left(\partial_i\varphi^T_C\right)\mathcal{C}_1 d\Omega \quad = \quad 0.
\end{aligned}\tag{57}$$

The final step is then to again assume the continuous flow perturbations are step-wise constant within each cell, and that $\delta U_p \approx \Delta U_p$, allowing them to be cancelled out. This gives the hybrid adjoint equation for viscous flow with a general turbulence model:

$$\begin{aligned}
&\int_{\Omega_p}\left(L^*_\Omega(\varphi_C)-\beta\left(\frac{\partial j_\Omega}{\partial U}\right)^T\right)d\Omega-(1-\beta)\sum_{q=1}^{N}\left(\frac{\mathfrak{D}j_q}{\mathfrak{D}U_p}\right)^T\Delta\Omega_q\\
&-\sum_{q=1}^{N}\left(\frac{\mathfrak{D}\mathcal{R}^{(*)}_{T_q}}{\mathfrak{D}U_p}\right)^T\varphi_{D_q}+\sum_{q=1}^{N}\left(\frac{\mathfrak{D}f_q}{\mathfrak{D}U_p}\right)^T\int_{\Omega_q}\mathcal{C}_1^T\partial_i\varphi_C d\Omega \quad = \quad 0.
\end{aligned}\tag{58}$$

With this definition, the perturbation to the objective function, given by eqn. (32) can thus be written

$$\begin{aligned}\{\delta,\Delta\}\mathcal{J}_H = \{\delta,\Delta\}\mathcal{L} \;=\; & \int_\Omega \left(\beta\frac{\partial j_\Omega}{\partial\alpha}\delta\alpha - \varphi_C^T\partial_i\left(\left(\frac{\partial F_i}{\partial\alpha} - \mathcal{A}_1 - \mathcal{A}_4 - \mathcal{B}_1\right)\delta\alpha\right)\right)d\Omega \\ & + \int_\Gamma \beta\frac{\partial j_\Gamma}{\partial\alpha}\delta\alpha d\Gamma + (1-\beta)\,\frac{\mathfrak{D}\mathcal{J}_D}{\mathfrak{D}\alpha}\Delta\alpha \\ & - \sum_{p=1}^{N}\frac{\mathfrak{D}f_p}{\mathfrak{D}\alpha}\Delta\alpha\int_{\Omega_p}\mathcal{C}_1^T\partial_i\varphi_C d\Omega + \sum_{p=1}^{N}\varphi_{D_p}^T\frac{\mathfrak{D}\mathcal{R}_{T_p}}{\mathfrak{D}\alpha}\Delta\alpha.\end{aligned} \tag{59}$$

B. Solution strategy

As for the flow, the solution method for the hybrid adjoint equations was implemented into the SU^2 CFD and design code.[40] In the same way as the primal problem, the adjoint was also solved by stepping through first the mean flow part and then the turbulence model part.

For the mean flow adjoint, the convective terms were discretized using the Jameson-Schmidt-Turkel central-differencing scheme (noting the absence of the shock-related artificial dissipation as no shocks are present in the adjoint solution) and the viscous terms were discretized through a combination of average gradients and piece-wise source terms, following the method used by Bueno-Orovio et al.[28] However, there were also additional discrete coupling terms added in as sources to the mean flow adjoint.

To obtain the required Jacobians for the turbulence variable-adjoint, the Spalart-Allmaras one-equation model routines from the flow solution method were differentiated using the TAPENADE AD tool.[19] Since SU^2 is written in C++ and TAPENADE works only on Fortran or C, this process was automated by creating a series of Python routines to convert the raw source code from C++ to C, run TAPENADE and then convert the differentiated routines back to C++. On the very first iteration of the hybrid adjoint code, a set of wrapping routines in SU^2 extracted the required discrete Jacobians from the differentiated code and stored them both to solve the adjoint turbulence model problem and to couple back into the mean flow adjoint equations.

Within each major iteration of the hybrid adjoint solver, an implicit backward Euler scheme was used for the pseudo-time integration of the mean flow step and then the turbulence model linear system was solved completely, noting that after each mean flow adjoint solution step the mixed coupling source term would alter this linear system.

V. Results

A. Theoretical analysis

Before applying the turbulent hybrid adjoint approach developed above to an appropriate test case, it is useful to first make some observations based on the theory:

1. The hybrid adjoint equations (58) are already written in finite volume form because of the need to discretize the domain integral.

2. Considering a continuous objective function defined on a surface, which does not explicitly depend on the turbulence model variables, such as the drag on an airfoil, and splitting equation (58) into the adjoint equations for the mean flow and for the turbulence model gives a continuous-like adjoint PDE with discrete and mixed source terms for the mean flow,

$$\int_{\Omega_p} L_\Omega^*(\varphi_C)d\Omega = \sum_{q=1}^{N}\left(\frac{\mathfrak{D}\mathcal{R}_{T_q}^{(*)}}{\mathfrak{D}U_p}\right)^T\varphi_{D_q} - \sum_{q=1}^{N}\left(\frac{\mathfrak{D}f_q}{\mathfrak{D}U_p}\right)^T\int_{\Omega_q}\mathcal{C}_1^T\partial_i\varphi_C d\Omega, \tag{60}$$

and a discrete-like linear system with mixed source terms for the turbulence model,

$$\sum_{q=1}^{N}\left(\frac{\mathfrak{D}\mathcal{R}_{T_q}^{(*)}}{\mathfrak{D}U_p}\right)^T\varphi_{D_q} = \sum_{q=1}^{N}\left(\frac{\mathfrak{D}f_q}{\mathfrak{D}U_p}\right)^T\int_{\Omega_q}\mathcal{C}_1^T\partial_i\varphi_C d\Omega, \tag{61}$$

noting that the chosen objective function influences the coupled system only through the hybrid boundary conditions on the viscous wall, i.e.,

$$\int_{S_p} \left(\frac{\partial j_\Gamma}{\partial p} - \varphi^T_{C_{\rho u_j}} \hat{n}_i \right) d\Gamma + \sum_{q=1}^{N_S} \varphi^T_{D_q} \left(\frac{\rho_p}{p_p} \frac{\mathfrak{D}(\hat{F}_T)_{\Gamma_q}}{\mathfrak{D}\rho_p} + \frac{1}{\gamma - 1} \frac{\mathfrak{D}(\hat{F}_T)_{\Gamma_q}}{\mathfrak{D}(\rho E)_p} \right) = 0, \tag{62}$$

$$\int_{S_p} \left(\frac{\partial j_\Gamma}{\partial T} + \left(\varphi^T_{C_{\rho u_j}} \tau_{ij} \frac{\partial \mu}{\partial T} + \mu \left(\partial_i \varphi_{C_{\rho E}} \right) \frac{C_p}{Pr} \right) \hat{n}_i \right) d\Gamma - \sum_{q=1}^{N_S} \frac{\rho_p}{T_p} \varphi^T_{D_q} \frac{\mathfrak{D}(\hat{F}_T)_{\Gamma_q}}{\mathfrak{D}\rho_p} = 0, \tag{63}$$

$$\int_{S_p} \left(\frac{\partial j_\Gamma}{\partial \tau_{ij}} + \varphi^T_{C_{\rho u_j}} \mu \hat{n}_i \right) d\Gamma = 0, \tag{64}$$

and

$$\sum_{q=1}^{N_S} \varphi^T_{D_q} \frac{\mathfrak{D}(\hat{F}_T)_{\Gamma_q}}{\mathfrak{D}U_{T_p}} = 0. \tag{65}$$

The form of equations (60) and (61) implies that the former should be solved as a PDE and the second as a linear system.

3. While the summation signs in the hybrid adjoint equations (58) and wall boundary conditions (54) are written as either over all the cells in the mesh, or all the cells along the surface, it is not typically required to consider the explicit dependence of every cell in the mesh to every other cell. The numerical scheme usually considers a smaller stencil for calculating the flow (and gradients) for any particular cell, and it is this stencil that is most important when handling parts of the hybrid approach discretely. The same is generally true of the calculation of the eddy viscosity.

4. The continuous-like treatment of the boundary conditions in the hybrid adjoint derivation implies that, at least on a viscous wall, the choice of objective function in the hybrid adjoint is restricted in a similar way as the continuous adjoint. This means that only functionals of the pressure, temperature, stress and turbulence adjoint variable should be considered. However, within the domain, there is the possibility of using a more varied selection of objective functions.

5. An important result from the hybrid derivation shown previously is that no derivatives of the eddy viscosity appear in the continuously-treated parts of the hybrid adjoint equations or boundary conditions, and instead these model-dependent derivatives are handled discretely. Since the turbulence model is treated discretely, and all required derivatives in the discrete implementation are derived using Automatic Differentiation (AD), this means that, given the only coupling from the turbulence model to the mean flow is via μ_T, the mathematical form of the hybrid adjoint is general for any turbulence model.

6. The derivation of the hybrid adjoint in this paper considered only viscous wall and far field boundary conditions. Some additional work therefore may be required to apply the resulting PDE to other boundary conditions, such as inlets and outlets, and if the outer boundary is not sufficiently far away that viscous terms cannot be neglected.

7. Though shape of the wall S was held fixed in the above derivations of the frozen-viscosity continuous adjoint and hybrid adjoint, the adjoint equations derived, and the adjoint variables that come from their solution, are in fact general and can be used to evaluate the sensitivities to changes in this shape. Assuming there is no explicit dependence of the objective function on the turbulence variables, the objective function depends only on the forces on S and some constant projection vector, and that the surface is either smooth or δS is zero where it is singular, it is possible to write the perturbation to

the objective function with respect to shape perturbations as[28]

$$\begin{aligned}\delta\mathcal{J} &= \int_S \left(\hat{n}_i \left(\partial_j \phi_{\rho u_i} + \partial_i \phi_{\rho u_j} - \frac{2}{3}\delta_{ij}\partial_l \phi_{\rho u_l} \right) \partial_k u_k \hat{n}_j \right. \\ &\quad \left. -\mu^{v2} C_p \left(\partial_i(\phi_{\rho E}) - \partial_j(\phi_{\rho E})\hat{n}_j\hat{n}_i\right)\left(\partial_i(T) - \partial_j(T)\hat{n}_j\hat{n}_i\right) \right) \delta S d\Gamma.\end{aligned} \tag{66}$$

This result can be used to evaluate the sensitivity of objective functions such as the coefficients of lift and drag on an airfoil with respect to changes in its surface shape.

B. Numerical results

The test cases used to investigate the frozen continuous and full hybrid adjoints were transonic flow over the RAE 2822 airfoil at non-zero angle-of-attack. The flow conditions used, corresponding to AGARD AR 138 cases 9 and 10,[23,24] were:

- Freestream Mach number, $M_\infty = 0.734$ (case 9) and $M_\infty = 0.754$ (case 10)
- Freestream temperature, $T_\infty = 273.15K$
- Angle-of-attack, $\alpha = 2.54^o$ (case 9) and $\alpha = 2.57^o$ (case 10)
- Reynolds number, $Re = 6.5 \times 10^6$ (case 9) and $Re = 6.2 \times 10^6$ (case 10)
- Gas constant, $R = 287.87 Jkg^{-1}K^{-1}$
- Ratio of specific heats, $\gamma = 1.4$

and the grid for this case contains a total of $13,937$ points, including 192 on the surface of the airfoil, and is given in Figure 3. The flow simulations were converged to machine precision (residual values of $1e^{-16}$), and the adjoint simulations until an approximation of the geometric sensitivity of the functional changed by less than $1e^{-6}$ over 100 iterations.

The turbulence model used was the Spalart-Allmaras one-equation turbulence model, and the resulting surface pressure coefficients are shown in Figures 4 and 5. The simulation of case 9 matches the pressure coefficients from experiment along the lower surface and upstream of the shock well, and also predicts the shock location. However, downstream of the shock there is a difference between the values obtained using simulation and experiment. Case 10 also shows good agreement on the lower surface, but on the upper surface the pressure coefficients from simulation and experiment now match more closely after the shock, whilst there is a difference between the shock location and values upstream.

1. *Surface sensitivity*

Figures 6 and 7 show the sensitivity of the coefficient of drag to changes in the surface of the RAE 2822 airfoil obtained using the frozen continuous and hybrid adjoint approaches for cases 9 and 10, respectively. It can be seen that for case 9 there is very little difference between the frozen continuous and hybrid results. For case 10, there is also no significant difference in the sensitivity on the lower surface, but on the upper surface, near the location of the shock, the frozen continuous and hybrid results noticeably differ. It should also be noted that for case 10 the drag is seen to be in general much more sensitive to changes on the upper surface, where the effects of turbulence are expected to be greatest.

2. *Shape sensitivity*

The airfoil shape was parameterized using 38 Hicks-Henne bump functions[41] and the sensitivity of the airfoil drag to changes in the surface was then calculated by projecting these bump functions onto the surface of the airfoil. These bumps were numbered from the lower side of the trailing edge clockwise towards the leading edge (0 to 18) and then backwards from the leading edge along the upper surface to the trailing edge (19 to 37), and positioned at intervals of 0.05 of the chord along the x-axis. The sensitivities obtained by finite differencing, the frozen-viscosity continuous adjoint and the hybrid adjoint are shown in Figures 8 and 9

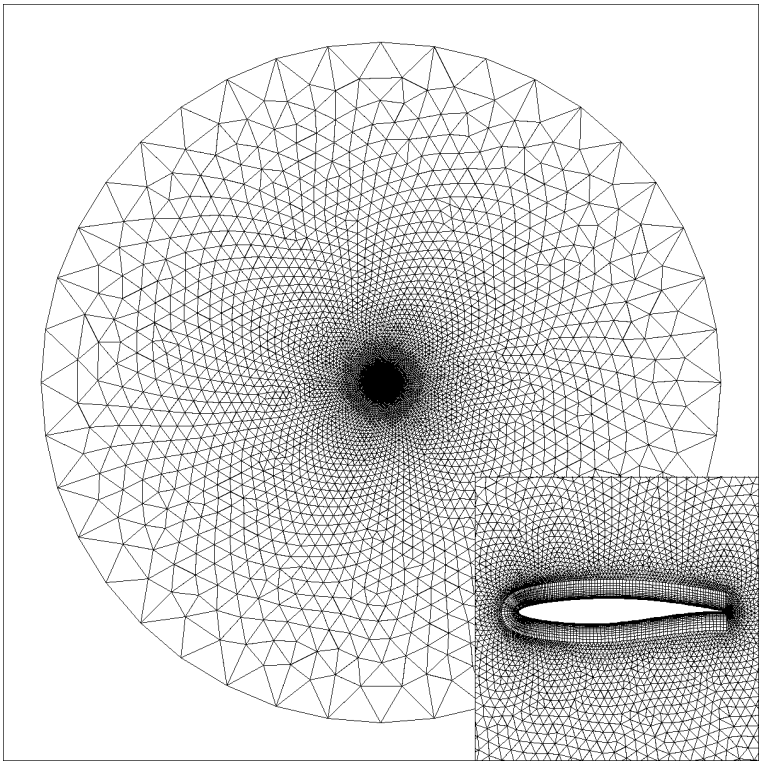

Figure 3. Computational mesh for the RAE 2822 airfoil used for the AGARD AR 138 turbulent flow cases 9 and 10.[23,24]

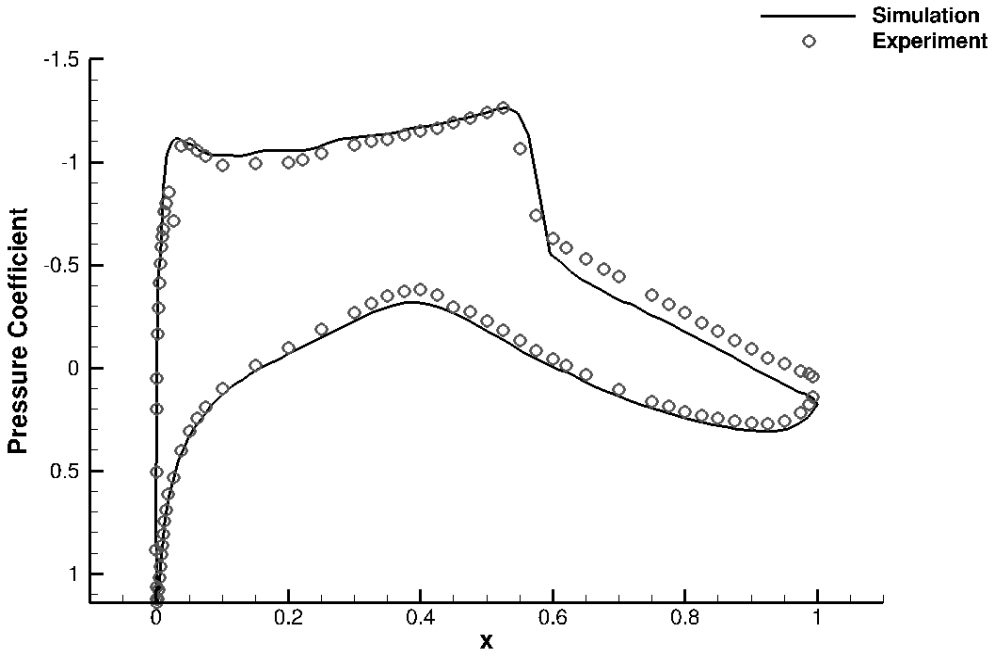

Figure 4. Pressure coefficient along the RAE 2822 airfoil for AGARD AR 138 case 9.[23]

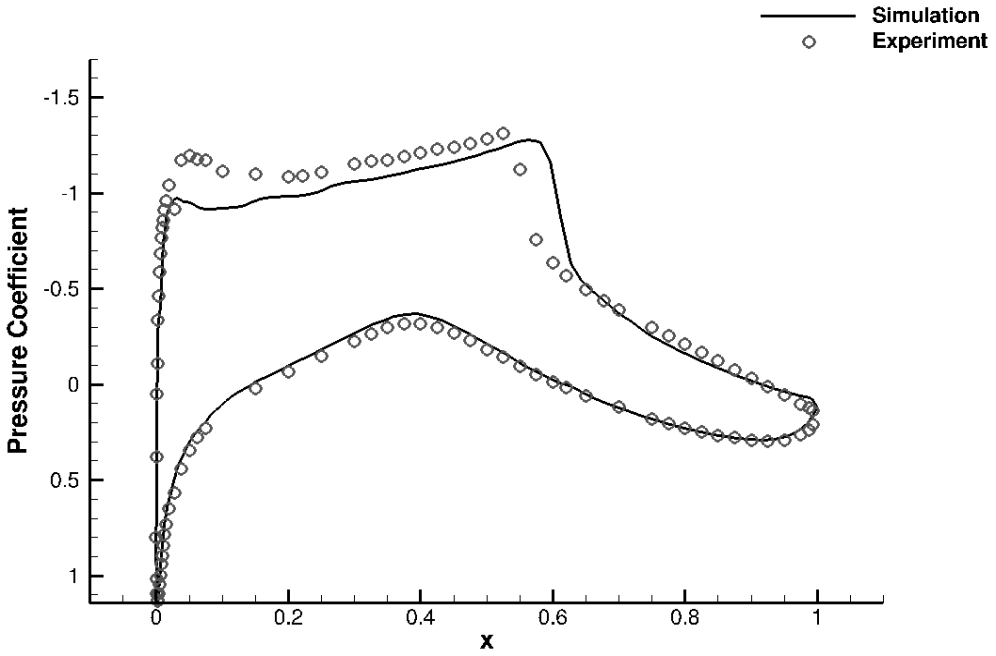

Figure 5. Pressure coefficient along the RAE 2822 airfoil for AGARD AR 138 case 10.[23]

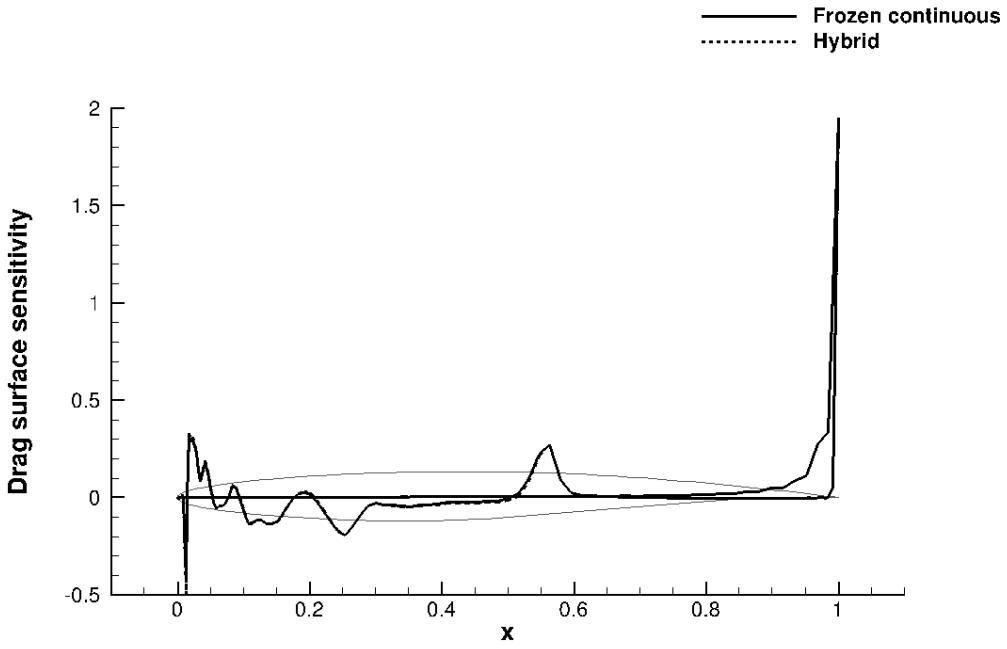

Figure 6. Surface sensitivity of coefficient of drag along the RAE 2822 airfoil for AGARD AR 138 case 9.[23]

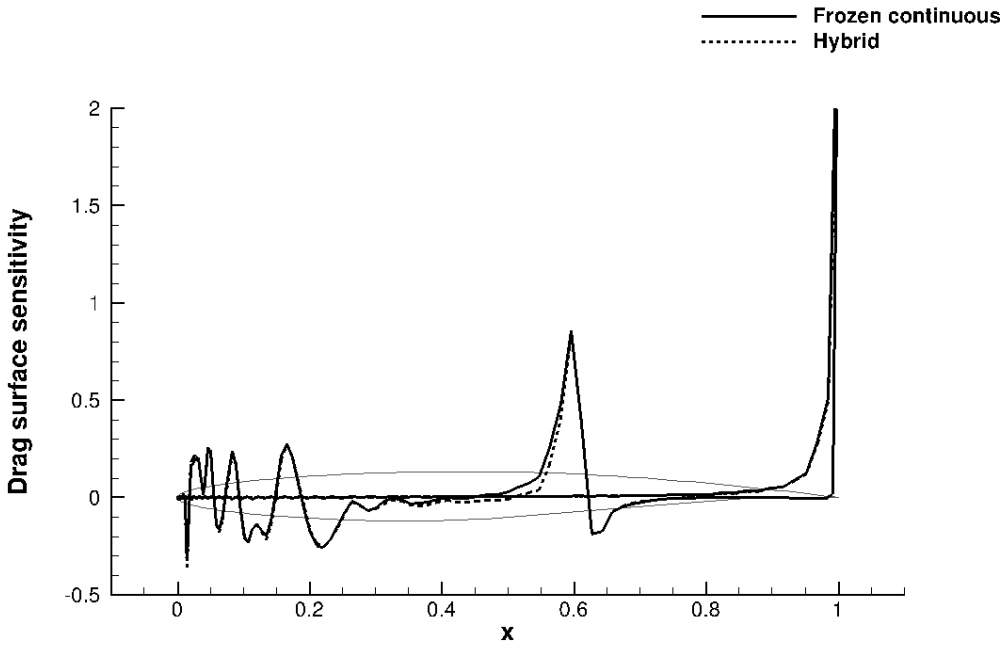

Figure 7. Surface sensitivity of coefficient of drag along the RAE 2822 airfoil for AGARD AR 138 case 10.[23]

for cases 9 and 10, respectively. For case 9, the two adjoints are seen to give relatively similar results, and neither agrees perfectly with finite differencing. For case 10, however, a marked difference is seen between the frozen-viscosity continuous adjoint, the hybrid adjoint and the results from finite differencing on the upper surface of the airfoil.

To validate the finite difference results for case 10, the finite difference step in the shape was varied from $1e^{-2}$ to $1e^{-8}$, but over this range no significant change was seen in the finite difference results.

3. Shape optimization

Using the above results for surface sensitivities, and the parametrization of the airfoil using 38 Hicks-Henne bump functions, both adjoint methods were then applied to a problem of gradient-based optimization of the shape of the RAE 2822 airfoil with the objective of reducing the drag, whilst keeping the lift constant. A simple quasi-newton method was used to enable the optimization.

Figures 10 and 11 show the evolution of the drag and lift values at each design step. Case 9 shows only a small difference between using the two adjoint approaches, as might be expected from the very similar surface sensitivities in Figure 6. After 10 design steps the frozen-viscosity continuous adjoint reduced the drag coefficient to 63.1% of the original value, increasing the lift-to-drag ratio to 73.2 (the baseline was 46.4). In comparison, the hybrid adjoint reduced the drag coefficient to 64.5% and raised the lift-to-drag ratio to 71.5.

Application of the hybrid adjoint to the optimization of case 10, however, showed a more significant difference from the frozen-viscosity continuous method. After 15 design steps the frozen-viscosity approach gave a drag coefficient of 53.1% of the original value with a lift-to-drag ratio of 55.6 (the baseline was 28.6), and the hybrid gave a drag coefficient of 48.4% and a lift-to-drag ratio of 61.8.

The resulting surface pressures are shown in Figures 12 and 13, indicating that the optimizer is able to reduce the strong shock on the upper surface. However, in case 10 the hybrid adjoint appears to have more substantially reduced the strength of the pressure jump on the upper surface of the airfoil than the frozen-viscosity continuous adjoint method.

The oscillatory nature of the coefficient of pressure profiles is expected to be caused by the relatively coarse discretization of the airfoil into 38 Hicks-Henne bump functions. Using a greater number of bumps

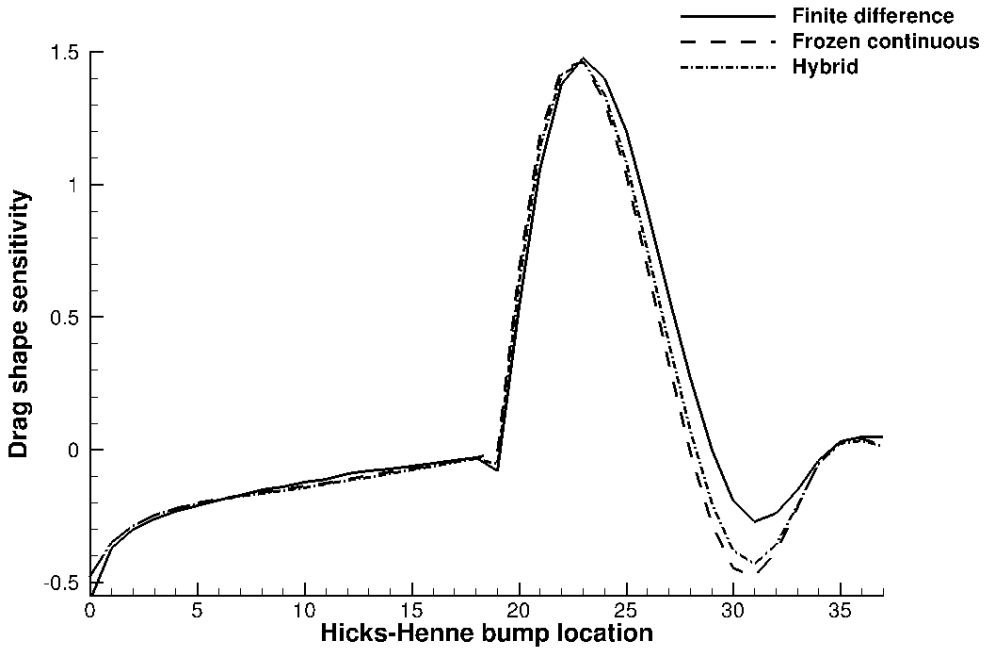

Figure 8. Shape sensitivity of coefficient of drag along the RAE 2822 airfoil for AGARD AR 138 case 9.[23]

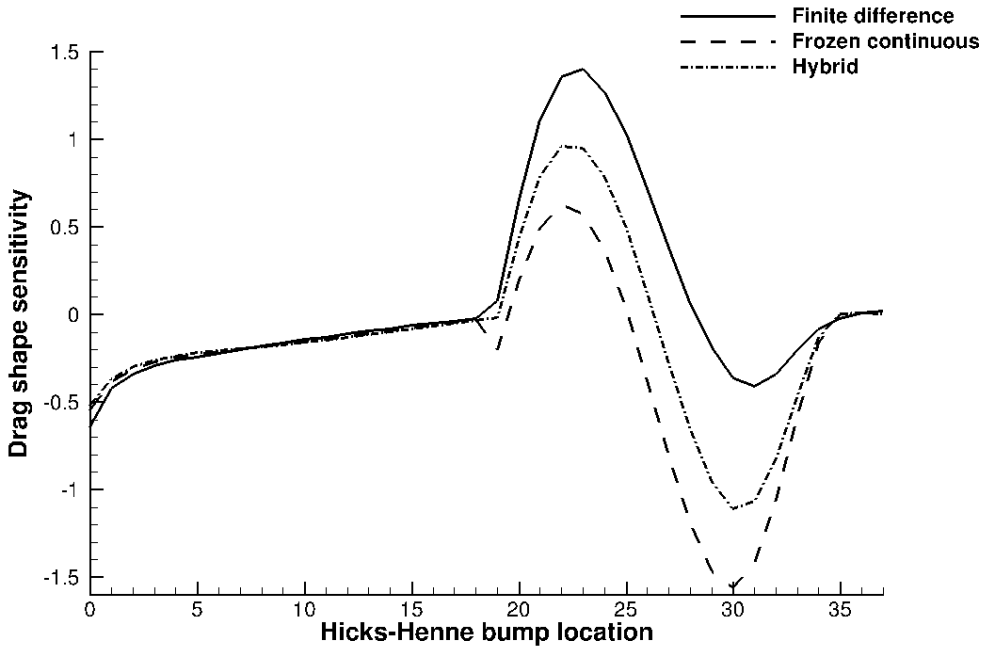

Figure 9. Shape sensitivity of coefficient of drag along the RAE 2822 airfoil for AGARD AR 138 case 10.[23]

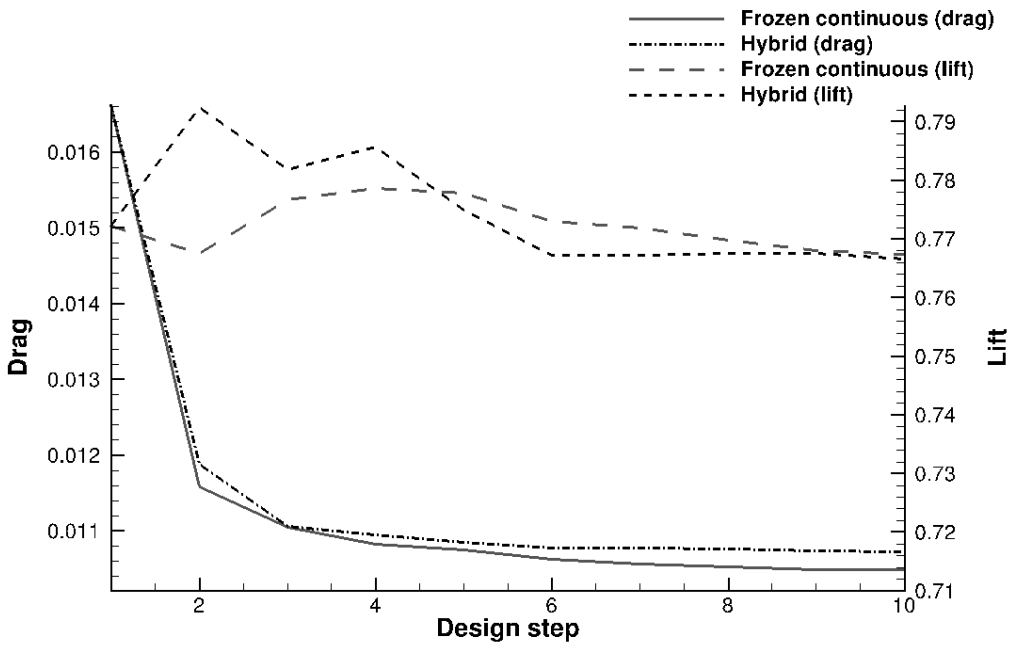

Figure 10. Shape optimization of the RAE 2822 airfoil for AGARD AR 138 case 9,[23] aiming to minimize the coefficient of drag whilst constraining the coefficient of lift above 0.77.

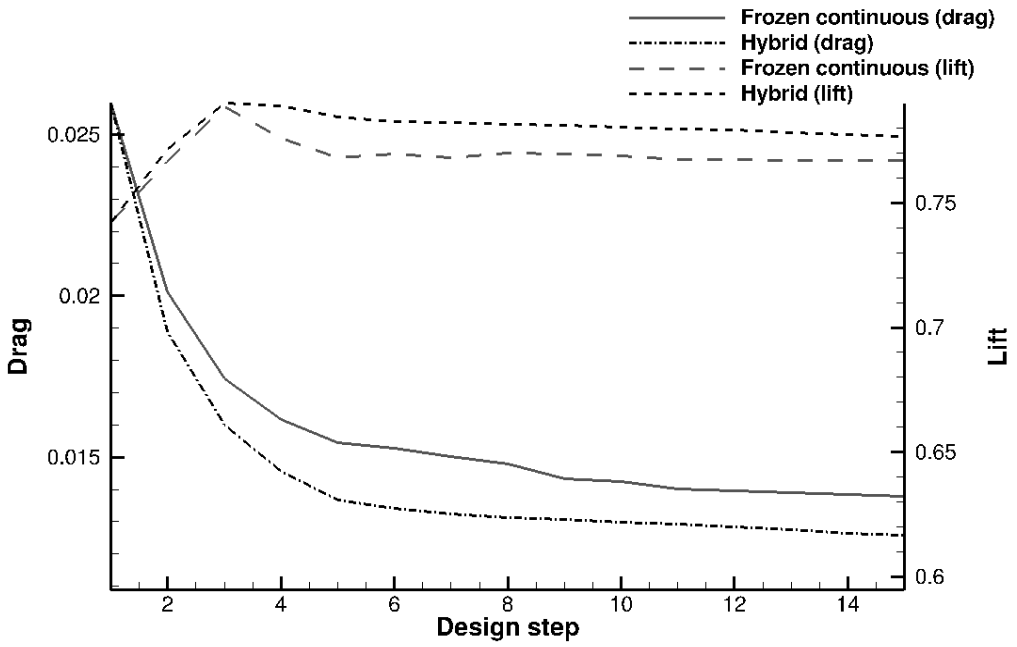

Figure 11. Shape optimization of the RAE 2822 airfoil for AGARD AR 138 case 9,[23] aiming to minimize the coefficient of drag whilst constraining the coefficient of lift above 0.74.

would be expected to smooth out the profiles.

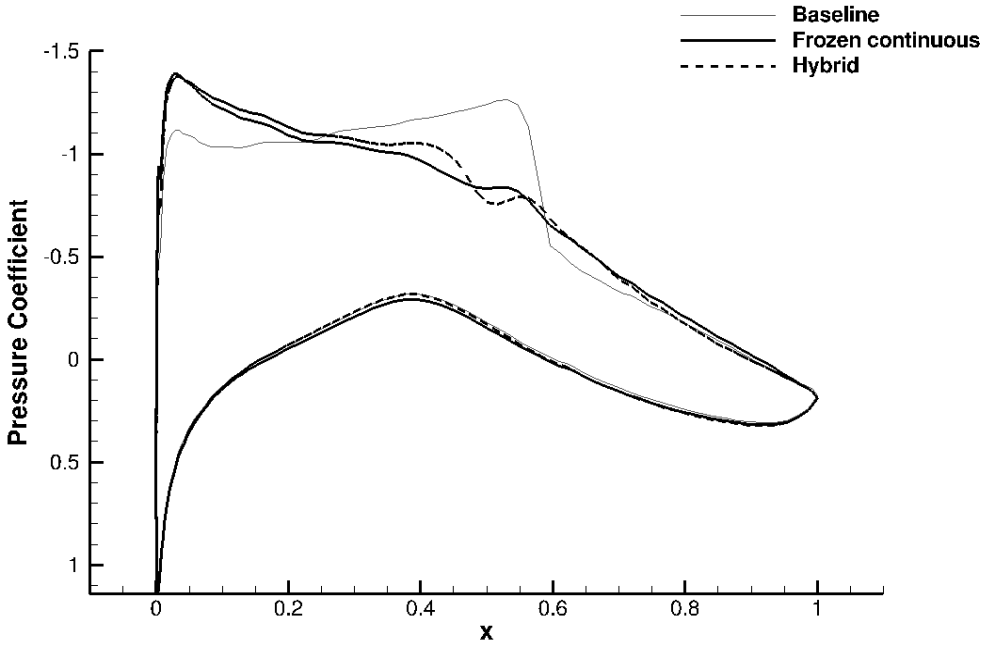

Figure 12. Coefficient of pressure along baseline and optimized (10th design step) RAE 2822 airfoils for AGARD AR 138 case 9.[23]

Finally, Figures 14 and 15 show the modified airfoil surfaces produced. Again, the difference between the frozen-viscosity and hybrid adjoint results for case 9 is small, but in the case 10 result it is possible to see a significant difference between the shapes produced on the upper surface of the airfoil.

VI. Conclusions and future work

The hybrid adjoint approach of Taylor et al. (2012) has been extended and applied to the compressible Reynolds Averaged Navier–Stokes (RANS) equations. The hybrid adjoint method treats the mean flow equations in a continuous sense and the turbulence model equations in a discrete sense. The formulation is devised such that the mathematical development is independent of the turbulence model. The key benefit is that by applying the discrete approach and Automatic Differentiation to handle arbitrarily complex terms in the turbulence model, mathematical difficulties may be circumvented, while the benefits of the continuous adjoint (such as consistency with the primal problem and reduced stiffness of the adjoint system) are retained. The formulation also handles the eddy viscosity term present in the continuously-treated mean flow equations in a discrete way, ensuring that this model-dependent coupling does not affect the generality of the hybrid adjoint development. The hybrid adjoint has been applied to a turbulent transonic flow over an airfoil and shape sensitivities are compared to finite differencing. As a demonstration test case, the hybrid adjoint is shown to enable a gradient-based shape optimization method to perform lift constrained drag minimization of the aforementioned transonic airfoil flow. When the effects of turbulence are small, relatively little difference is seen between the frozen-viscosity continuous adjoint and the hybrid adjoint, but where the effects become significant, using the hybrid produces a lower value of the drag coefficient for a set number of iterations.

Acknowledgments

This work is funded through the United States Department of Energy's Predictive Science Academic Alliance Program at Stanford University.

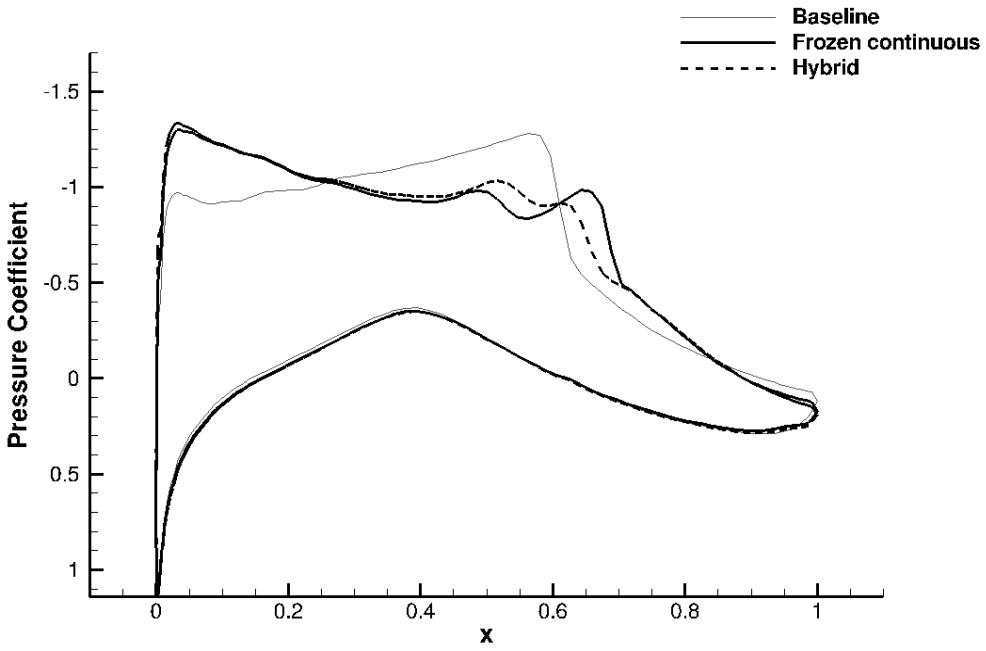

Figure 13. Coefficient of pressure along baseline and optimized (15th design step) RAE 2822 airfoils for AGARD AR 138 case 10.[23]

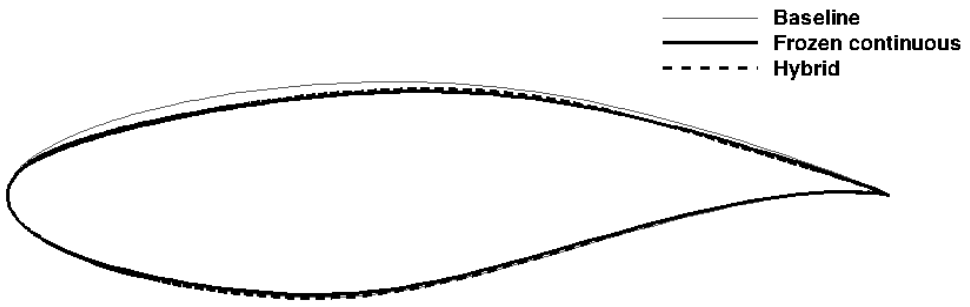

Figure 14. Shape comparison of baseline and optimized (10th design step) RAE 2822 airfoils for AGARD AR 138 case 9.[23] Note that the shape has been stretched so that $x : y = 0.5 : 1$ to make the shape differences clearer.

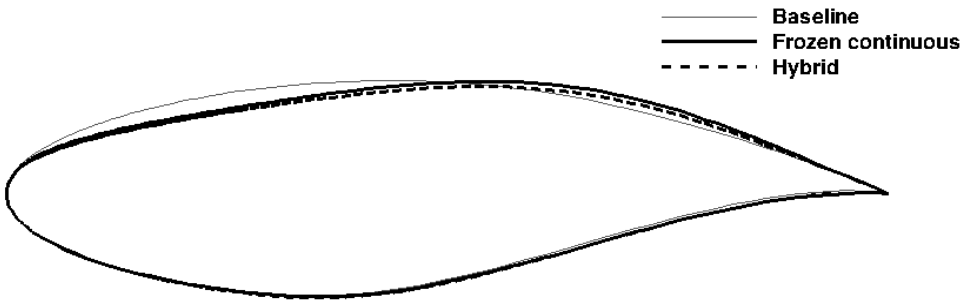

Figure 15. Shape comparison of baseline and optimized (10th design step) RAE 2822 airfoils for AGARD AR 138 case 10.[23] Note that the shape has been stretched so that $x : y = 0.5 : 1$ to make the shape differences clearer.

References

[1]Jameson, A., "Aerodynamic Design via Control Theory," *Journal of Scientific Computing*, Vol. 3, No. 3, 1988, pp. 233–260.

[2]Lions, J. L., *Optimal Control of Systems Governed by Partial Differential Equations*, Springer Verlag, New York, 1971.

[3]Reuther, J. and Jameson, A., "Supersonic Wing and Wing-Body Shape optimization Using an Adjoint Formulation," *International Mechanical Engineering Congress and Exposition*, 1995.

[4]Jameson, A. and Alonso, J. J., "Aerodynamic Shape Optimization Techniques Based On Control Theory," *AIAA*, 1998.

[5]Reuther, J. J., Jameson, A., Alonso, J. J., Rimlinger, M. J., and Saunders, D., "Constrained Multipoint Aerodynamic Shape Optimization Using an Adjoint Formulation and Parallel Computers, Part 1," *Journal of Aircraft*, Vol. 36, No. 1, January-February 1999, pp. 51–60.

[6]Reuther, J. J., Jameson, A., Alonso, J. J., Rimlinger, M. J., and Saunders, D., "Constrained Multipoint Aerodynamic Shape Optimization Using an Adjoint Formulation and Parallel Computers, Part 2," *Journal of Aircraft*, Vol. 36, No. 1, January-February 1999, pp. 61–74.

[7]Baysal, O. and Eleshaky, M. E., "Aerodynamic Sensitivity Analysis Methods for the Compressible Euler Equations," *Journal of Fluids Engineering*, Vol. 113, 1991, pp. 681–688.

[8]Martins, J. R. R. A. and Hwang, J. T., "Review and Unification of Methods for Computing Derivatives of Multidisciplinary Systems," *53rd AIAA/ASME/ASCE/AHS/ASC Structures, Structural Dynamics and Materials Conference*, Honolulu, HI, April 2012.

[9]Duraisamy, K. and Alonso, J. J., "Adjoint Based Techniques for Uncertainty Quantification in Turbulent Flows with Combustion," *42nd AIAA Fluids Dynamics Conference*, New Orleans, LA, June 2012.

[10]Duraisamy, K. and Chandrashekar, P., "Goal-oriented uncertainty propagation using stochastic adjoints," *Computers and Fluids*, Vol. 66, 2012, pp. 10–20.

[11]Palacios, F., Duraisamy, K., Alonso, J. J., and Zuazua, E., "Robust Grid Adaptation for Efficient Uncertainty Quantification," *AIAA Journal*, Vol. 50, No. 7, 2012, pp. 1538–1546.

[12]Pierce, N. A. and Giles, M. B., "Adjoint and defect error bounding and correction for functional estimates," *Journal of Computational Physics*, Vol. 200, 2004, pp. 769–794.

[13]Giles, M. B., Duta, M. C., Müller, J.-D., and Pierce, N. A., "Algorithm Developments for Discrete Adjoint Methods," *AIAA Journal*, Vol. 41, No. 2, 2003, pp. 198–205.

[14]Venditti, D. A. and Darmofal, D. L., "Anisotropic Grid Adaptation for Functional Outputs: Application to Two-dimensional Viscous Flows," *Journal of Computational Physics*, Vol. 187, 2002, pp. 22–46.

[15]Giles, M. B. and Pierce, N. A., "On the Properties of Solutions of the Adjoint Euler Equations," *Numerical Methods for Fluid Dynamics*, Vol. IV, 1998, pp. 1–16.

[16]Giles, M. B. and Pierce, N. A., "Improved lift and drag estimates using adjoint Euler equations," *AIAA*, 1999.

[17]Nemec, M., Aftosmis, M. J., and Wintzer, M., "Adjoint-Based Adaptive Mesh Refinement for Complex Geometries," *46th AIAA Aerospace Sciences Meeting*, Reno, NV., January 2008.

[18]Wintzer, M., Nemec, M., and Aftosmis, M. J., "Adjoint-Based Adaptive Mesh Refinement for Sonic Boom Prediction," *26th AIAA Applied Aerodynamics Conference*, Honolulu, HI, August 2008.

[19]Hascoët, L. and Pascual, V., "TAPENADE 2.1 user's guide," Technical Report 0300, INRIA, http://www.inria.fr/rrrt/rt-0300.html, 2004.

[20]Griewank, A., Juedes, D., and Utke, J., "Algorithm 755: ADOL-C: A Package for the Automatic Differentiation of Algorithms Written in C/C++," *ACM Transactions on Mathematical Software*, Vol. 22, No. 2, 1996, pp. 131–167.

[21]Nadarajah, S. K. and Jameson, A., "A Comparison of the Continuous and Discrete Adjoint Approach to Automatic Aerodynamic Optimization," *38th AIAA Aerospace Sciences Meeting*, No. AIAA-2000-0667, Reno, NV., January 2000.

[22]Taylor, T. W. R., Palacios, F., Duraisamy, K., and Alonso, J. J., "Towards a Hybrid Adjoint Approach for Arbitrarily Complex Partial Differential Equations," *42nd AIAA Fluids Dynamics Conference*, New Orleans, LA, June 2012.

[23]Cook, P. H., McDonald, M. A., and Firmin, M. C. P., "Aerofoil RAE 2822 — Pressure Distributions, and Boundary Layer and Wake Measurements," Advisory Report 138, AGARD, 1979.

[24]Haase, W., Bradsma, F., Elsholz, E., Leschziner, M., and Schwamborn, D., editors, *EUROVAL: An European Initiative on Validation of CFD Codes*, Vol. 42, Wiley, New York, 1993.

[25]Giles, M. B., Ghate, D., and Duta, M. C., "Using Automatic Differentiation for Adjoint CFD Code Development," Technical Report 05/25, Oxford University Computing Laboratory, 2005.

[26]Giles, M. B. and Pierce, N. A., "An Introduction to the Adjoint Approach to Design," *Flow, Turbulence and Combustion*, Vol. 65, 2000, pp. 393–415.

[27]Mader, C. A., Martins, J. R. R. A., Alonso, J. J., and Weide, E. V. D., "ADjoint: An Approach for the Rapid Development of Discrete Adjoint Solvers," *AIAA Journal*, Vol. 46, April 2008, pp. 4.

[28]Bueno-Orovio, A., Castro, C., Palacios, F., and Zuazua, E., "Continuous Adjoint Approach for the Spalart-Allmaras Model in Aerodynamic Optimization," *AIAA Journal*, Vol. 50, No. 3, March 2012.

[29]Lozano, C. and Ponsin, J., "Remarks on the numerical solution of the adjoint quasi-one-dimensional Euler equations," *International Journal for Numerical Methods in Fluids*, Vol. 69, 2011, pp. 966–982.

[30]Castro, C., Lozano, C., Palacios, F., and Zuazua, E., "Systematic Continuous Adjoint Approach to Viscous Aerodynamic Design on Unstructured Grids," *AIAA Journal*, Vol. 45, No. 9, September 2007, pp. 2125–2139.

[31]Baeza, A., Castro, C., Palacios, F., and Zuazua, E., "2D Euler Shape Design on Non-Regular Flows Using Adjoint Rankine-Hugoniot Relations," *AIAA Journal*, Vol. 47, No. 3, March 2009, pp. 522–562.

[32]Nielsen, E. J. and Anderson, W. K., "Aerodynamic Design Optimization on Unstructured Meshes Using the Navier-Stokes Equations," *AIAA*, 1998.

[33]Belegundu, A. D. and Arora, J. S., "A Sensitivity Interpretation of Adjoint Variables in Optimal Design," *Computer Methods in Applied Mechanics and Engineering*, Vol. 48, 1985, pp. 81–89.

[34]Anderson, W. K. and Venkatakrishnan, V., "Aerodynamic Design Optimization on Unstructured Grids with a Continuous Adjoint Formulation," *Computers and Fluids*, Vol. 28, No. 4-5, May-June 1999, pp. 443–480.

[35]Taylor, T. W. R., Palacios, F., Duraisamy, K., and Alonso, J. J., "Towards a hybrid adjoint approach for complex flow simulations," *Center for Turbulence Research Annual Research Briefs*, 2012, pp. 333–345.

[36]Taylor, T. W. R., *A Hybrid Adjoint Approach for Systems of Arbitrarily Complex Partial Differential Equations*, Ph.D. thesis, Stanford University, 2013.

[37]Giles, M. B., Duta, M. C., Müller, J.-D., and Pierce, N. A., "Algorithm Developments for Discrete Adjoint Methods," *AIAA Journal*, Vol. 41, No. 2, 2003, pp. 198–205.

[38]Wilcox, D. C., *Turbulence Modeling for CFD*, DCW Industries, 3rd ed., 2006.

[39]Spalart, P. R. and Allmaras, S. R., "A One-equation Turbulence Model for Aerodynamic Flows," *La Recherche Aerospatiale*, 1994.

[40]Palacios, F., Colonno, M. R., Aranake, A. C., Campos, A., Copeland, S. R., Economon, T. D., Lonkar, A. K., Lukaczyk, T. W., Taylor, T. W. R., and Alonso, J. J., "Stanford University Unstructured (SU2): An open-source integrated computational environment for multi-physics simulation and design," *51st AIAA Aerospace Sciences Meeting*, Grapevine, TX, January 2013.

[41]Hicks, R. M. and Henne, P. A., "Wing Design by Numerical Optimization," *Journal of Aircraft*, Vol. 15, No. 7, 1978, pp. 407–412.